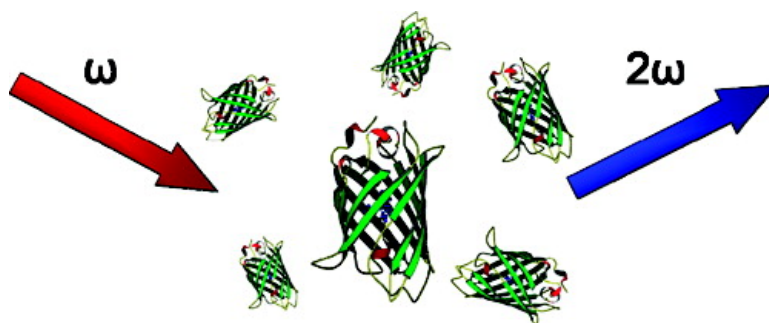Article

Second-Harmonic Generation in GFP-like Proteins

Inge Asselberghs, Cristina Flors, Lara Ferrighi, Edith Botek, Benoi#t Champagne, Hideaki Mizuno, Ryoko Ando, Atsushi Miyawaki, Johan Hofkens, Mark Van der Auweraer, and Koen Clays

More About This Article

Additional resources and features associated with this article are available within the HTML version:

- Supporting Information
- Access to high resolution figures
- Links to articles and content related to this article
- Copyright permission to reproduce figures and/or text from this article

View the Full Text HTML

Second-Harmonic Generation in GFP-like Proteins

Inge Asselberghs,[†] Cristina Flors,*,[†,ll] Lara Ferrighi,[‡] Edith Botek,[‡]
Benoît Champagne,[‡] Hideaki Mizuno,[§] Ryoko Ando,[§] Atsushi Miyawaki,[§]
Johan Hofkens,[†] Mark Van der Auweraer,[†] and Koen Clays*,[†]

*Department of Chemistry and Institute for Nanoscale Physics and Chemistry (INPAC),
Katholieke Universiteit Leuven, Celestijnenlaan 200D and F, B-3001 Leuven, Belgium, Facultés
Universitaires Notre Dame de la Paix, Namur, Belgium, and Laboratory for Cell Function and
Dynamics, Brain Science Institute, RIKEN, 2-1 Hirosawa, Wako, Saitama 351-0198, Japan*

Received July 4, 2008; E-mail: cristina.flors@ed.ac.uk; koen.clays@fys.kuleuven.be

Abstract: The second-order nonlinear optical properties of green fluorescent proteins (GFPs), such as
the photoswitchable Dronpa and enhanced GFP (EGFP), have been studied at both the theoretical and
experimental levels. In the case of Dronpa, both approaches are consistent in showing the rather
counterintuitive result of a larger second-order nonlinear polarizability (or first hyperpolarizability, β) for the
protonated state, which has a higher transition energy, than for the deprotonated, fluorescent state with its
absorption at lower energy. Moreover, the value of β for the protonated form of Dronpa is among the highest
reported for proteins. In addition to the pH dependence, we have found a wavelength dependence in the
β values. These properties are essential for the practical use of Dronpa or other GFP-like fluorescent proteins
as second-order nonlinear fluorophores for symmetry-sensitive nonlinear microscopy imaging and as
nonlinear optical sensors for electrophysiological processes. An accurate value of the first hyperpolarizability
is also essential for any qualitative analysis of the nonlinear images.

Introduction

Dronpa is a protein from the green fluorescent protein (GFP) family derived from a Pectiniidae coral.[1] As in the case of other GFP-like proteins, its structure consists of a central chromophore that is formed autocatalytically by the cyclization of a tripeptide, which is placed in a characteristic 11-stranded β-barrel.[2,3] The chromophore consists of a phenol group conjugated to an imidazolinone group, with highly polarizable electrons (A in Chart 1).[4] The significance of Dronpa stems from its ability to reversibly photoswitch between a bright fluorescent state and a dark state with good efficiency when irradiated with 488 and 405 nm light. Photoswitching involves an interplay between proton transfer and light-dependent regulation of its structural flexibility that brings about changes in the geometry of the chromophore and the protein environment, including chromophore isomerization.[5-7] Dronpa photoswitching has been demonstrated at the ensemble and single-molecule levels.[1,8-10]

The photoswitching capability of Dronpa might be useful not only for its application in fluorescence-tracking experiments but also in a more general way that profits from the possibility of controlling by light the switching between two different species, one protonated (neutral) and one deprotonated (anionic). This structural difference might also induce a difference in other physicochemical parameters, in particular, nonlinear optical (NLO) properties, since its structure is noncentrosymmetric. The different ionization states of the two forms, and thus their

different ground and excited states and transition dipole moments, suggest that their NLO properties will differ. Examples of compounds with (photo)switchable NLO properties can be found in the literature; these involve switching by pH changes,[11] electrochemical potential,[12-14] or light.[15-18] However, the

(1) Ando, R.; Mizuno, H.; Miyawaki, A. *Science* **2004**, *306*, 1370–1373.
(2) Stiel, A. C.; Trowitzsch, S.; Weber, G.; Andresen, M.; Eggeling, C.; Hell, S. W.; Jakobs, S.; Wahl, M. C. *Biochem. J.* **2007**, *402*, 35–42.
(3) Wilmann, P. G.; Turcic, K.; Battad, J. M.; Wilce, M. C. J.; Devenish, R. J.; Prescott, M.; Rossjohn, J. *J. Mol. Biol.* **2006**, *364*, 213–224.
(4) Niwa, H.; Inouye, S.; Hirano, T.; Matsuno, T.; Kojima, S.; Kubota, M.; Ohashi, M.; Tsuji, F. I. *Proc. Natl. Acad. Sci. U.S.A.* **1996**, *93*, 13617–13622.
(5) Fron, E.; Flors, C.; Schweitzer, G.; Habuchi, S.; Mizuno, H.; Ando, R.; Miyawaki, A.; de Schryver, F. C.; Hofkens, J. *J. Am. Chem. Soc.* **2007**, *129*, 4870–4871.
(6) Andresen, M.; Stiel, A. C.; Trowitzsch, S.; Weber, G.; Eggeling, C.; Wahl, M. C.; Hell, S. W.; Jakobs, S. *Proc. Natl. Acad. Sci. U.S.A.* **2007**, *104*, 13005–13009.
(7) Mizuno, H.; Mal, T. K.; Walchli, M.; Kikuchi, A.; Fukano, T.; Ando, R.; Jeyakanthan, J.; Taka, J.; Shiro, Y.; Ikura, M.; Miyawaki, A. *Proc. Natl. Acad. Sci. U.S.A.* **2008**, *105*, 9227–9232.
(8) Habuchi, S.; Ando, R.; Dedecker, P.; Verheijen, W.; Mizuno, H.; Miyawaki, A.; Hofkens, J. *Proc. Natl. Acad. Sci. U.S.A.* **2005**, *102*, 9511–9516.
(9) Habuchi, S.; Dedecker, P.; Hotta, J.; Flors, C.; Ando, R.; Mizuno, H.; Miyawaki, A.; Hofkens, J. *Photochem. Photobiol. Sci.* **2006**, *5*, 567–576.
(10) Dedecker, P.; Hotta, J.; Ando, R.; Miyawaki, A.; Engelborghs, Y.; Hofkens, J. *Biophys. J.* **2006**, *91*, L45–L47.
(11) Asselberghs, I.; Zhao, Y.; Clays, K.; Persoons, A.; Comito, A.; Rubin, Y. *Chem. Phys. Lett.* **2002**, *364*, 279–283.
(12) Asselberghs, I.; Clays, K.; Persoons, A.; Ward, M. D.; McCleverty, J. *J. Mater. Chem.* **2004**, *14*, 2831–2839.
(13) Coe, B. J. *Acc. Chem. Res.* **2006**, *39*, 383–393.
(14) Asselberghs, I.; Clays, K.; Persoons, A.; McDonagh, A. M.; Ward, M. D.; McCleverty, J. A. *Chem. Phys. Lett.* **2003**, *368*, 408–411.

† Katholieke Universiteit Leuven.
‡ Facultés Universitaires Notre Dame de la Paix.
§ RIKEN Brain Science Institute.
ll Present address: University of Edinburgh, School of Chemistry, Kings Buildings, West Mains Rd., EH9 3JJ Edinburgh, U.K.

Chart 1. Successive Models of the GFP Chromophore and Its Surroundings (the Bottom Picture Corresponds to the Two Forms of Model D in Equilibrium)
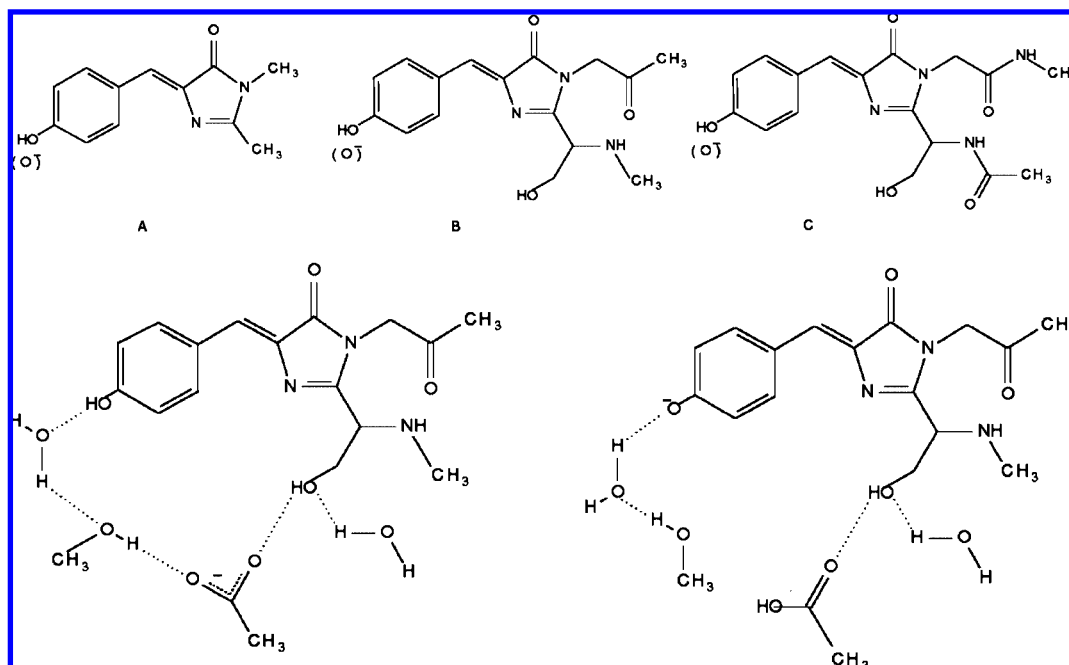
ability to genetically encode Dronpa into a biological system is a clear advantage compared to ordinary organic molecules.

In this paper, we report on the capability of the two forms of Dronpa to generate second-harmonic light, which is a property of interest for its applicability in second-harmonic imaging microscopy (SHIM).[19] SHIM is based on the interaction between short pulses of IR or NIR light and asymmetrically distributed molecules to produce light at twice the frequency of the incident light with an intensity dependence on the induced dipole moment. It has already been shown that irradiation of GFP with 100 ps pulses at 1064 nm produces a second-harmonic signal with sufficient intensity to be used in SHIM of living cells.[20,21] GFP that is targeted to a membrane can change its second-harmonic generation (SHG) capability in response to changes in membrane potential and other electrophysiological phenomena.[20,21] More recently, video-rate nonlinear microscopy based on GFP as nonlinear contrast agent, which involves scanning the focused illuminating spot derived from a femtosecond laser emitting at 910 nm, has been reported.[22] SHIM can be a complement of multiphoton fluorescence microscopy (MPFM)[23,24] and provide information on protein localization

together with data on functional responses associated with behavioral and sensory processes. Femtosecond pulses have the inherent advantage of higher peak power, resulting in more efficient nonlinear conversion of the fundamental to both MPFM and SHIM.

Since the use and the interpretation of second-order nonlinear images depends on both the value of the first hyperpolarizability β at the molecular level and the symmetry of the arrangement of the molecules at the bulk level, a study of the value of β is deemed essential for the correct interpretation of second-harmonic images. We have explored the effect of pH and wavelength on β as important factors for the potentially quantitative evaluation of what to date has been the qualitative interpretation of the MPF and SHG images. For this study, we have used hyper-Rayleigh scattering (HRS), which is the incoherent second-order nonlinear light scattering at the second-harmonic wavelength, to which the equivalent linear version is the simple Rayleigh scattering at the fundamental, impinging wavelength. It should be noted that the alternative experimental technique for determining the first hyperpolarizability β, namely, electric-field-induced SHG, is not applicable in the case of ionic chromophores or proteins. Even at the isoelectric point of proteins, the electric field that is used to induce the noncentrosymmetry by dipolar orientation orients proteins on the basis of the charge distribution over the protein rather than on the basis of the chromophore dipole moment.[25,26] HRS takes advantage of the local deviations (in both time and space) from the average noncentrosymmetry.[27−29] Since GFPs are highly

(15) Lai, N. D.; Wang, W. L.; Lin, J. H.; Hsu, C. C. *Appl. Phys. B: Lasers Opt.* **2005**, *80*, 569–572.

(16) Sanguinet, L.; Pozzo, J. L.; Rodriguez, V.; Adamietz, F.; Castet, F.; Ducasse, L.; Champagne, B. *J. Phys. Chem. B* **2005**, *109*, 11139–11150.

(17) Sliwa, M.; Letard, S.; Malfant, I.; Nierlich, M.; Lacroix, P. G.; Asahi, T.; Masuhara, H.; Yu, P.; Nakatani, K. *Chem. Mater.* **2005**, *17*, 4727–4735.

(18) Sekkat, Z.; Knoesen, A.; Lee, V. Y.; Miller, R. D. *J. Phys. Chem. B* **1997**, *101*, 4733–4739.

(19) Campagnola, P. J.; Loew, L. M. *Nat. Biotechnol.* **2003**, *21*, 1356–1360.

(20) Lewis, A.; Khatchatouriants, A.; Treinin, M.; Chen, Z. P.; Peleg, G.; Friedman, N.; Bouevitch, O.; Rothman, Z.; Loew, L.; Sheres, M. *Chem. Phys.* **1999**, *245*, 133–144.

(21) Khatchatouriants, A.; Lewis, A.; Rothman, Z.; Loew, L.; Treinin, M. *Biophys. J.* **2000**, *79*, 2345–2352.

(22) Roorda, R. D.; Hohl, T. M.; Toledo-Crow, R.; Miesenbock, G. *J. Neurophysiol.* **2004**, *92*, 609–621.

(23) Mohler, W.; Millard, A. C.; Campagnola, P. J. *Methods* **2003**, *29*, 97–109.

(24) Moreaux, L.; Sandre, O.; Blanchard-Desce, M.; Mertz, J. *Opt. Lett.* **2000**, *25*, 320–322.

(25) Birge, R. R.; Fleitz, P. A.; Lawrence, A. F.; Masthay, M. A.; Zhang, C. F. *Mol. Cryst. Liq. Cryst.* **1990**, *189*, 107–122.

(26) Clays, K.; Hendrickx, E.; Triest, M.; Verbiest, T.; Persoons, A.; Dehu, C.; Bredas, J. L. *Science* **1993**, *262*, 1419–1422.

(27) Clays, K.; Persoons, A. *Phys. Rev. Lett.* **1991**, *66*, 2980–2983.

(28) Clays, K.; Persoons, A. *Rev. Sci. Instrum.* **1992**, *63*, 3285–3289.

fluorescent, the HRS signal at the second-harmonic wavelength has contributions from both incoherent scattering and multiphoton fluorescence. A number of techniques have been proposed to eliminate this source of systematic error (overestimation of β due to the MPF contribution to the HRS signal). These techniques can involve the spectral domain (based on the difference between the narrow spectral peak for HRS at exactly the second-harmonic wavelength and the broad emission spectrum as a background),[30] the time domain (based on the difference between the instantaneous scattering and the time-delayed fluorescence),[31] and the frequency domain. This last technique is basically the Fourier transform of the approach in the time domain. For high amplitude-modulation (AM) frequencies, the fluorescence can no longer follow the fast excitation and is thus no longer modulated. This demodulation, or decrease in amplitude for higher AM frequencies, represents the modulus of the response along the real and imaginary parts of the Fourier transforms.[32] There is also a functional dependence for the phase that the signal acquires (the phase angle in complex space for the Fourier transforms). From the data analysis of both demodulation and phase as a function of AM frequency, it is possible to extract the fluorescence-free value of β (as the high-frequency limit), the multiphoton fluorescence contribution, and the fluorescence lifetime.[33]

In addition to Dronpa, we have examined two model compounds to aid in the interpretation of our HRS data: the nonphotoswitchable enhanced GFP (EGFP), which is deprotonated at the pH used, and the isolated GFP chromophore 4-hydroxybenzylidene-1,2-dimethylimidazolinone (HBDI) (A in Chart 1). Quantum-chemical calculations were also carried out at different levels of sophistication, which were applied to different protein models varying from a simplified chromophore to one in which the interaction with its environment was taken into account. These calculations give additional support to the presented experimental data.

Experimental Section

Materials. Dronpa was expressed and purified as described previously.[1] The buffers used were 50 mM TRIS (pH 8.0) and 50 mM phosphate−citrate (pH 5.0) (Aldrich) and 50 mM citrate, glycine, and NaH_2PO_4 adjusted to pH 4 with concentrated HCl. Photoconversion of Dronpa was achieved by illuminating the solution at 488 nm with a continuous-wave (CW) Ar−Kr ion laser (Stabilite 2018-RM, Spectra Physics) until total photoconversion was achieved. Reconversion was easily achieved by daylight illumination at room temperature until complete recovery was obtained. The EGFP vector was purchased from Clontech Laboratories Inc. HBDI was synthesized as described previously.[34]

Instrumentation. The hyper-Rayleigh scattering experiments were performed as described in detail by Olbrechts et al.[32] In this work, operating output wavelengths of the Ti:sapphire laser (Spectra-Physics) of 840 and 880 nm were used to perform the measurement. The appropriate bandpass filters (420 and 440 nm)

(CVI, 10 nm bandwidth) were placed in front of the photomultiplier. At each modulation frequency the apparent hyperpolarizability $\beta_{HRS,app}$ was calculated from the measurements of a dilution series of the protein in the appropriate buffer solution. The individual buffer solutions were checked and did not produce additional signals interfering with the measurements. From a simultaneous fit of $\beta_{HRS,app}$ and the phase difference $\Delta\varphi$, the fluorescence-free hyperpolarizability β_{HRS} and fluorescence lifetime τ were obtained.[33] From the accurate, multiphoton fluorescence-free β_{HRS}, the major contributing tensor component assuming molecular $C_{\infty v}$ symmetry (i.e., β_{zzz}, where the unique molecular axis is the z axis) was calculated using $\beta_{HRS} = (^6/_{35})^{1/2}\beta_{zzz}$.[35] To confirm our assumption about the symmetry of the nonlinear scatterer, HRS depolarization measurements were performed.[36] The ratio ρ of the parallel- and perpendicular-polarized HRS intensities (with the polarization directions defined with respect to the incoming, vertically polarized fundamental along the laboratory Z axis), defined as

$$\rho = \frac{\langle\beta_{ZZZ}^2\rangle}{\langle\beta_{ZXX}^2\rangle}$$

is sensitive to the different contributions of the various nonzero tensor components and therefore to the symmetry of the scatterer. Purely dipolar scatterers, for which only β_{zzz} contributes to the signal, have a ρ value of 5 in the limit of pure molecular $C_{\infty v}$ symmetry and finite numerical aperture, while, for example, octopolar symmetries give $\rho = 1.5$. For a real dipolar molecule, experimental ρ values of ∼3 have been found, in agreement with the nonzero off-diagonal tensor components found in real molecules.

Although the two-level model is not applicable for extracting accurate, absolute values for dispersion-free hyperpolarizabilities close to resonance,[37] it can be used to derive an estimate for the relative enhancement effect when moving to a slightly different fundamental wavelength only. To assess the relative importance of the damping, which is not included in the simple two-level model, we also report our estimates including damping factors, as estimated from the width of the absorption peaks.

As an external reference, crystal violet (CV) in methanol solution was measured at the same input wavelength. The literature reports an octopolar hyperpolarizability $\beta_{xxx} = 338 \times 10^{-30}$ esu at 800 nm. This reference value was also converted to values at 840 and 880 nm by applying the two-level model.[37] The recalculated hyperpolarizabilities are $\beta_{xxx}(CV, 840 \text{ nm}) = 367 \times 10^{-30}$ esu and $\beta_{xxx}(CV, 880 \text{ nm}) = 413 \times 10^{-30}$ esu.

Theoretical Methods. The HRS first hyperpolarizability and the absorption spectra were calculated for successive models of the chromophore and its surroundings, whose structures were optimized using density functional theory (DFT) with the B3LYP exchange-correlation (XC) functional and the 6-311G** basis set, without any symmetry restrictions. The HRS quantities are reported for the static case ($\lambda = \infty$) as well as accounting for frequency dispersion ($\lambda = 1064$ and 800 nm) as

$$\beta_{HRS} = \sqrt{\langle\beta_{ZZZ}^2\rangle + \langle\beta_{ZXX}^2\rangle}$$

Full expressions without assuming Kleinman's conditions were used to determine the $\langle\beta_{ZZZ}^2\rangle$ and $\langle\beta_{ZXX}^2\rangle$ HRS components.[38] The Moller−Plesset perturbation theory approach limited to second order (MP2) was applied in combination with the finite-field procedure to determine the static first hyperpolarizability tensor. The accuracy of the numerical derivatives was improved by employing the

(29) Clays, K.; Persoons, A.; De Maeyer, L. *Adv. Chem. Phys.* **1994**, *85*, 455–498.

(30) Hsu, C. C.; Shu, C. F.; Huang, T. H.; Wang, C. H.; Lin, J. L.; Wang, Y. K.; Zang, Y. L. *Chem. Phys. Lett.* **1997**, *274*, 466–472.

(31) Noordman, O. F. J.; vanHulst, N. F. *Chem. Phys. Lett.* **1996**, *253*, 145–150.

(32) Olbrechts, G.; Strobbe, R.; Clays, K.; Persoons, A. *Rev. Sci. Instrum.* **1998**, *69*, 2233–2241.

(33) Wostyn, K.; Binnemans, K.; Clays, K.; Persoons, A. *Rev. Sci. Instrum.* **2001**, *72*, 3215–3220.

(34) Kojima, S.; Ohkawa, H.; Hirano, T.; Maki, S.; Niwa, H.; Ohashi, M.; Inouye, S.; Tsuji, F. I. *Tetrahedron Lett.* **1998**, *39*, 5239–5242.

(35) Cyvin, S. J.; Rauch, J. E.; Decius, J. C. *J. Chem. Phys.* **1965**, *43*, 4083–4095.

(36) Heesink, G. J. T.; Ruiter, A. G. T.; van Hulst, N. F.; Bolger, B. *Phys. Rev. Lett.* **1993**, *71*, 999–1002.

(37) Oudar, J. L.; Chemla, D. S. *J. Chem. Phys.* **1977**, *66*, 2664–2668.

(38) Bersohn, R.; Pao, Y. H.; Frisch, H. L. *J. Chem. Phys.* **1966**, *45*, 3184–3198.

Table 1. Hyperpolarizability Measured for Dronpa by Hyper-Rayleigh Scattering at Fundamental Wavelengths of 840 and 880 nm

	840 nm					880 nm	
	pH 8	pH 5	pH 4	pH 8 photoswitched	pH 8 reconverted	pH 8	pH 4
λ_{max} (nm)	503	388	381	387	503	503	381
β_{HRS} (10^{-30} esu)	245 ± 22	693 ± 68	1033 ± 89	419 ± 20	359 ± 15	332 ± 12	780 ± 44
$\beta_{0,HRS}$ (10^{-30} esu)[a]	68 ± 7	74 ± 7	111 ± 10		72 ± 2	68 ± 3	134 ± 8
$\beta_{0,HRS}$ (10^{-30} esu)[b]	72 ± 7		318 ± 28			76 ± 3	255 ± 14
β_{zzz} (10^{-30} esu)	594 ± 59	1673 ± 166	2494 ± 214	1012 ± 48	866 ± 36	804 ± 30	1883 ± 106
$\beta_{0,zzz}$ (10^{-30} esu)	165 ± 16	180 ± 19	269 ± 23		174 ± 10	166 ± 6	324 ± 18
τ_{fluor} (ns)[c]	4.9 ± 2.6	n.d.	n.d.	n.d.	3.9 ± 2.6	n.d.	n.d.

[a] Static hyperpolarizability calculated using the classical two-state model of Oudar and Chemla.[37] [b] Static hyperpolarizability calculated using damping factors (4800 and 2000 cm^{-1} fwhm for the protonated and deprotonated forms, respectively). [c] n.d. = no MPF detected at the second-harmonic wavelength.
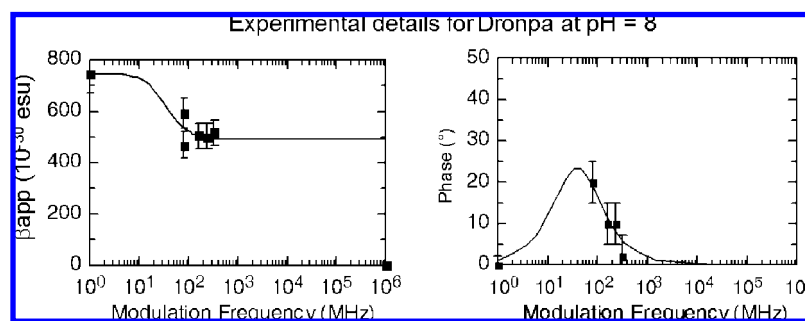

Figure 1. (left) Demodulation and (right) phase as a function of AM frequency for Dronpa at pH 8 and incident wavelength 840 nm. The solid squares represent the measured data points, and the solid line is the fit to a model containing a single-exponential-decay multiphoton fluorescence contribution on top of a frequency-independent nonlinear scattering background.

Romberg procedure. The frequency-dependent β_{HRS} values were obtained using the multiplicative approximation scheme

$$\beta_{MP2}(-2\omega;\omega,\omega) \approx \beta_{MP2}(0;0,0)\frac{\beta_{TDHF}(-2\omega;\omega,\omega)}{\beta_{CPHF}(0;0,0)}$$

where the frequency dispersion is estimated to be similar at the Hartree−Fock (HF) and MP2 levels.[39−41] This approach enables both electron correlation and dispersion effects to be taken into account. The time-dependent Hartree-Fock (TDHF) and coupled-perturbed Hartree−Fock (CPHF) schemes provide dynamic and static HF hyperpolarizabilities, respectively, using procedures involving analytical differentiation of the wave function with respect to the external electric field.

The absorption spectra were simulated from the vertical excitation energies and related oscillator strengths determined using the time-dependent DFT (TDDFT) approach with the same B3LYP XC functional, an approach that has been shown to be efficient for determining the excitation energies of a broad range of organic compounds and in particular to reproduce changes in spectra upon structure modifications.[42−44] A Gaussian line shape with a fwhm of 0.13 eV was assumed for each transition.

All of the calculations employed the 6-311G** basis set. All of the geometry optimizations and property calculations were carried out using the Gaussian03 suite of programs,[45] except for the

evaluation of the TDDFT first hyperpolarizabilities, which was done with the Dalton package.[46]

Results and Discussion

Experimental Results. The first hyperpolarizability values for the two forms of Dronpa, protonated and deprotonated, were measured in solution by means of HRS. Deprotonated Dronpa was measured in TRIS buffer at pH 8 (pK_a = 5).[1] The protonated form was generated in two ways: reducing the solution pH and photoswitching at pH 8 (see the absorption spectra in Figure SI2 in the Supporting Information). Table 1 shows the results for the measured first hyperpolarizability β_{HRS}, β_{zzz}, the fluorescence lifetime retrieved from the demodulation analysis (see the Experimental Section), and the absorption maxima under the different conditions described above. β_{HRS} corresponds to the averaged hyperpolarizability, which is independent of the symmetry of the measured protein. To calculate the value of β_{zzz}, a molecular $C_{\infty v}$ symmetry was assumed. This assumption was confirmed by depolarization measurements (see below). Additionally, the dispersion-free hyperpolarizability $\beta_{0,HRS}$ and $\beta_{0,zzz}$ were calculated using the classical two-state model, as described by Oudar and Chemla.[37] We also estimated the effect of the damping by taking into account the widths (fwhm) of the absorption spectra, which had values of 4800 and 2000 cm^{-1} for the protonated and deprotonated forms, respectively. It should be noted that these widths were only estimates, especially for the deprotonated form, which has an absorption band that is not symmetric.

For deprotonated Dronpa at pH 8 with irradiation at 840 nm, demodulation due to the detected two-photon fluorescence at the second-harmonic wavelength (420 nm) was observed. The

(39) Rice, J. E.; Handy, N. C. *Int. J. Quantum Chem.* **1992**, *43*, 91–118.
(40) Sekino, H.; Bartlett, R. J. *Chem. Phys. Lett.* **1995**, *234*, 87–93.
(41) Jacquemin, D.; Champagne, B.; Hattig, C. *Chem. Phys. Lett.* **2000**, *319*, 327–334.
(42) Champagne, B.; Guillaume, M.; Zutterman, F. *Chem. Phys. Lett.* **2006**, *425*, 105–109.
(43) Rappoport, D.; Furche, F. *J. Am. Chem. Soc.* **2004**, *126*, 1277–1284.
(44) Homem-de-Mello, P.; Mennucci, B.; Tomasi, J.; da Silva, A. B. F. *Theor. Chem. Acc.* **2005**, *113*, 274–280.
(45) Frisch, M. J.; et al. Gaussian 03, revision C.02; Gaussian, Inc.: Wallingford, CT, 2004.

(46) DALTON: A Molecular Electronic Structure Program, release 2.0 (2005). http://www.kjemi.uio.no/software/dalton/dalton.html. (accessed Oct 17, 2008).

experimentally obtained apparent hyperpolarizability and phase data as a function of the AM frequency are shown in Figure 1. Because of the relatively long fluorescence lifetime, a complete demodulation of the hyperpolarizability can be reached within the bandwidth of the experiment (1 GHz). This is observed as the leveling off of the apparent hyperpolarizability for the highest AM frequencies. Consistent with this, the phase between the total nonlinear scattering signal and the reference also tends to zero for the highest AM frequencies. At high AM frequencies, the fluorescence is completely demodulated (it does not contribute to the signal anymore), and only instantaneous scattering contributes to the signal, which results in a phase shift of zero. The retrieved fluorescence lifetime is consistent with that obtained from time-correlated single-photon counting (3.6 ns),[8] taking into consideration the differences between our experimental conditions and those in ref 8.

It is apparent from Table 1 that protonated Dronpa has higher β values than the deprotonated form. In Dronpa at pH 4, in which ~90% of the chromophore is protonated, this value is 4-fold higher than in Dronpa at pH 8, in which the chromophore is deprotonated. The solution at pH 5 (50% protonated) confirms this tendency. From the value of β_{HRS} for the deprotonated form (245×10^{-30} esu) and the ratios of protonated to deprotonated Dronpa at the measured pH values, we can estimate β_{HRS} for the pH-induced protonated form as ~1150×10^{-30} esu. The higher hyperpolarizability values are thus observed in conjunction with the higher electronic transition energy (shorter wavelength of absorption), i.e., for the protonated form. This is in contrast with what would be expected from the simple two-level model, which predicts a larger hyperpolarizability for smaller transition energies. Interestingly, the photoswitched protonated form (~90% photoconversion) shows a statistically significantly lower β value than its pH-induced counterpart (pH 4) (Table 1), although that value is still higher than for the deprotonated form. We confirmed that the original values retrieved at pH 8 could be recovered upon reconversion of photoswitched Dronpa (Table 1).

The different values of β for the two protonated forms emphasize the difference between them, which has also been revealed by other spectroscopic experiments.[5,8] Since the chromophore structure should be identical in both protonated forms, a different arrangement of the protein environment or a different chromophore conformation is probably the reason for this difference. X-ray data suggest that photoswitched protonated Dronpa adopts a loose conformation that can accommodate a trans noncoplanar chromophore with a twist angle of ~30°,[6] but to date there is no published information about the structure of the pH-induced protonated from. Differences in the coplanarity of the hydroxyphenyl and imidazolinone moieties of the chromophore in the different forms of protonated Dronpa could be a reason for the observed behavior. Chromophore coplanarity has recently been recognized as an important factor in the contribution to β,[47] as it is also crucial for the fluorescence in GFP-like proteins.[48,49]

To clarify the reasons for the difference between the SHG capabilities of the protonated and deprotonated forms, depo-

(47) Perez-Moreno, J.; Asselberghs, I.; Song, K.; Clays, K.; Zhao, Y. X.; Nakanishi, H.; Okada, S.; Nogi, K.; Kim, O. K.; Je, J.; Matrai, J.; De Maeyer, M.; Kuzyk, M. G. *J. Chem. Phys.* **2007**, *126*, 074705.
(48) Prescott, M.; Ling, M.; Beddoe, T.; Oakley, A. J.; Dove, S.; Hoegh-Guldberg, O.; Devenish, R. J.; Rossjohn, J. *Structure* **2003**, *11*, 275–284.
(49) Henderson, J. N.; Remington, S. J. *Physiology* **2006**, *21*, 162–170.

Table 2. Results of the Depolarization Measurements at 840 nm for Dronpa under Different Environmental Conditions

| | ρ | | | |
modulation frequency (MHz)	pH 8 (fluorescent)	pH 4	photoconverted	CV (octopolar)
0.001	2.02	2.73	2.60	1.42
80	2.41	2.65	2.45	1.42
160[a]	n.m.	3.10	n.m.	1.57
240	2.80	2.80	2.90	1.43

[a] n.m. = not measured.

Table 3. HRS Results for Various Proteins

	EGFP	bR	bilirubin	HSA	collagen
reference	this work	26	50	50	51
operating wavelength (nm)	800	1064	1064	1064	1064
λ_{max} (nm)	488	570	432	280	
β_{HRS} (10^{-30} esu)	321 ± 31	910	89 ± 2	182 ± 4	99
$\beta_{0,HRS}$ (10^{-30} esu)		96	25 ± 1.5	120 ± 2	
β_{zzz} (10^{-30} esu)	776 ± 75	2200	215 ± 5	430 ± 10	240
$\beta_{0,zzz}$ (10^{-30} esu)		231	61 ± 3	289 ± 7	

larization experiments (Table 2) were performed. The results show that the depolarization ratio converges in each case to the same value of 2.8 as the fluorescence contribution is demodulated at sufficiently high AM frequency (240 MHz). This implies that the observed trend in the hyperpolarizabilities of Dronpa in the different protonation states cannot be attributed to symmetry changes of the chromophore and thus should reflect the different protein environments.

We also investigated the effect that changing the irradiation wavelength has on the values of β and the relative difference between the protonation states of Dronpa (Table 1), since the magnitude of the SHG intensity can be enhanced when the second-harmonic frequency is in resonance with an electronic absorption band.[19] We thus chose 880 nm, for which the second harmonic is closer to the absorption band of the deprotonated form. At this wavelength, β_{HRS} has the values (332 ± 12) $\times$ 10^{-30} and (780 ± 44) $\times 10^{-30}$ esu at pH 8 and 4, respectively. Thus, the tendency for β is similar at 840 nm, and no other enhancement than that due to resonance was found, since similar static hyperpolarizabilities were obtained at the two operating wavelengths. If the damping effect is neglected, these values amount to (68 ± 3) $\times 10^{-30}$ and (134 ± 8) $\times 10^{-30}$ esu at pH 8 and 4, respectively. With the estimates for the damping effect included, the values revert to 76×10^{-30} and 255×10^{-30} esu at pH 8 and 4, respectively. Thus, the resonance enhancement effect can be excluded as an explanation of the larger hyperpolarizability value for the protonated Dronpa with higher transition energy.

We also measured the second-harmonic generation ability of EGFP, which is a deprotonated nonphotoswitchable GFP-like protein, in order to use it as a model for our observations (Table 3). Our results on EGFP are indeed very similar to those measured for deprotonated Dronpa, i.e., $\beta_{HRS} \approx 300 \times 10^{-30}$ esu for both EGFP (at 800 nm) and Dronpa (at 840 and 880 nm). This means that the structural differences between the chromophores of EGFP and Dronpa, which involve the presence of a cysteine in the chromophore tripeptide in Dronpa instead of a threonine residue,[2,3] do not introduce an appreciable difference in their nonlinear optical response. Attempts to measure the β values for the isolated model chromophore HBDI (A in Chart 1) in its protonated (pH 5) and deprotonated (1 M NaOH) forms were made, but we were unable to detect any

Table 4. Theoretical HRS First Hyperpolarizabilities β_{HRS} (au) and Depolarization Ratios ρ (in Parentheses) for GFP Chromophore Models A and B in Their Protonated and Deprotonated Forms; Amplitudes of the β_{HRS} Response for Models D, E, and F (see the Supporting Information) Relative to the Corresponding β_{HRS} Value for Model B Are Also Given[a]

	MP2		HF		TDDFT/B3LYP	
	$\lambda = \infty$	$\lambda = 1064$ nm	$\lambda = \infty$	$\lambda = 1064$ nm	$\lambda = \infty$	$\lambda = 1064$ nm
	Model A: β_{HRS} (ρ)					
protonated	1208 (4.79)	1761	697 (4.30)	1017 (4.50)	1088 (4.63)	2014 (4.82)
deprotonated	1348 (4.71)	2300	1336 (4.11)	2332 (4.44)	908 (5.16)	1999 (5.31)
R	0.90	0.77	0.51	0.44	1.20	1.01
	Model B: β_{HRS} (ρ)					
protonated	1544 (4.89)	2286	851 (4.52)	1260 (4.67)	1275 (4.16)	2356 (4.12)
deprotonated	715 (5.42)	1176	1243 (4.20)	2046 (4.53)	1019 (5.95)	2812 (4.08)
R	2.16	1.94	0.68	0.62	1.25	0.84
	Model D: β_{HRS}(D)/β_{HRS}(B)					
protonated	−	−	1.53	1.27	1.26	1.41
deprotonated	−	−	1.52	1.67	1.48	1.34
	Model E: β_{HRS}(E)/β_{HRS}(B)					
protonated	−	−	1.37	1.47	1.35	1.55
deprotonated	−	−	1.52	1.70	1.28	1.11
	Model F: β_{HRS}(F)/β_{HRS}(B)					
protonated	−	−	−	−	−	−
deprotonated	−	−	1.75	1.92	2.02	1.91

[a] The calculations were performed at the HF, MP2, and TDDFT/B3LYP levels of theory using the 6-311G** basis set. R is the β_{HRS}(protonated)/β_{HRS}(deprotonated) ratio.

HRS signal stronger than that produced by the solvent blank at 840 or 880 nm irradiation or even at the higher excitation intensities provided by a nanosecond Nd:YAG laser at 1064 nm. This suggests that the protein matrix in Dronpa has a dramatic influence on the high β values found.

Besides the values measured in this work for EGFP, Table 3 contains values of β extracted from literature for other proteins: bacteriorhodopsin (bR),[26] bilirubin,[50] human serum albumin (HSA)[50] and collagen.[51] As these data indicate, the second-order nonlinear optical properties of (protonated) Dronpa are among the highest reported for proteins. It is important to note that the complete demodulation of our data assures that our results are free from the contribution of fluorescence. It is remarkable how retinal, the free chromophore of bR, varies depending on solvent and protonation state, with values ranging from 270×10^{-30} esu (free retinal in chloroform at 1064 nm) to 3600×10^{-30} esu (protonated retinal Schiff base in methanol at 1064 nm),[52] reflecting an effect of the protein environment on the SHG ability of the chromophore similar to that for GFP-like proteins.

Theoretical Results. For the calculations of the NLO properties, we chose several models having increasing levels of complexity, which take into account not only the central chromophore but also some important surrounding amino acids. The models represent GFP-like proteins in general rather than being specific to Dronpa and are mostly based on the wild-type GFP (wt-GFP) structure.

The main model systems considered in the present work can be obtained from Chart 1. Model A presents only the central part of the chromophore and is equivalent to HBDI, the model chromophore used in the above experimental studies. Model B is obtained by substituting the methyl groups on the imidazolinone with the more realistic side chains of the Gly67 and Ser65

residues (numbering as in wt-GFP). Moreover, since in the GFP, Gly67 and Ser65 are bonded to Val68 and Phe64, respectively, through amino−carbonyl bonds, we also considered model C, where the side chains have been further extended.[53] The next model (D) is more complex: it includes not only the main chromophore but also the molecules directly involved in the hydrogen-bonding network responsible for the proton transfer between Tyr66 and Ser65. In this case, more detailed representations of the protonated and deprotonated forms are given in Chart 1. The residues Ser205 and Glu222 are represented by a methanol and an acetic acid molecule, respectively, the latter being present in its deprotonated form in the case of the protonated chromophore. Both forms of model D therefore have a negative total charge of −1. Even more complex models have been envisaged and have been invoked to substantiate the calculations on the smaller models and to explain the observed experimental results (see the Supporting Information).

The calculated HRS data are listed in Table 4. These data can be analyzed as a function of each of the following: the inclusion of electron correlation, the increasingly more accurate description of the GFP chromophore environment, and the protonation state. At the MP2 level of approximation ($\lambda = \infty$ nm), the ratio R, defined as β_{HRS}(protonated)/β_{HRS}(deprotonated), amounts to 0.90 and 2.16 for models A and B, respectively, demonstrating that model B is at least required to reproduce the experimental result. It should be noted that the HF approach leads to the wrong relative amplitudes of the β_{HRS} responses for both models A and B, whereas the TDDFT/B3LYP calculations do not evidence any impact of the model, though the ratio is slightly larger than one. Frequency dependence as included at the TDHF and TDDFT levels even worsens the agreement between theory and experiment with respect to R. As judged from the data, ρ is not a good indicator of the protonation state, since its value is in all cases close to 5, which is typical for a dipolar chromophore. Moreover, the variations with the method of calculation are at least as large as those due

(50) Ranjini, A. S.; Das, P. K.; Balaram, P. J. Phys. Chem. B **2005**, 109, 5950–5953.

(51) Shcheslavskiy, V. I.; Petrov, G. I.; Yakovlev, V. V. Chem. Phys. Lett. **2005**, 402, 170–174.

(52) Hendrickx, E.; Clays, K.; Persoons, A.; Dehu, C.; Bredas, J. L. J. Am. Chem. Soc. **1995**, 117, 3547–3555.

(53) El Yazal, J.; Prendergast, F. G.; Shaw, D. E.; Pang, Y. P. J. Am. Chem. Soc. **2000**, 122, 11411–11415.

to the protonation state. It is worthy of note that we also tested the effect of replacing the O atom corresponding to Ser65 in model B by a S atom (corresponding to Cys62 in the Dronpa chromophore),[3] and the results were similar (data not shown).

From a more technical point of view, the inclusion of electron correlation effects at the MP2 level leads to an increase in the HRS responses (with respect to the HF values) of the protonated form by 73 and 81% for models A and B, respectively. On the other hand, for the deprotonated form, the effects of electron correlation are modified and inverted. In particular, the static HRS response of the deprotonated form decreases by 42% for model B in going from HF to MP2. This appears to be associated with the anionic nature of the chromophore. Moreover, the corresponding TDDFT/TDHF ratios amount to 0.66 and 0.82 for models A and B, respectively. It is further interesting to notice that at the TDHF level, the frequency dispersion of β_{HRS} before the first transition is well-reproduced by considering the two-state approximation.[37]

As was done in earlier work,[54−56] these first hyperpolarizability results were correlated to geometrical parameters, in particular, the bond-length alternation (BLA) of the conjugated segment between the two rings of the chromophore (see the Supporting Information). At the B3LYP/6-311G** level of approximation, the BLA amounts to 0.093 and 0.021 Å for the protonated and deprotonated forms of model A, whereas the corresponding values for model B are 0.090 and 0.012 Å. This demonstrates that the deprotonation is accompanied by a substantial increase of the conjugation along the chain, which is also associated with an important quinonoid character of Tyr66 and a reduction of the first hyperpolarizability. A different point of view from which to analyze the differences between the first hyperpolarizabilities of the protonated and deprotonated forms consists of resorting to the summation-over-states expression. In the two-state approximation, the dominant longitudinal component is $\beta_{zzz} = 3\mu_{0e}^2(\mu_{ee} - \mu_{00})/\Delta E_{0e}^2$, where μ_{e0} is the transition dipole moment between states e and 0, ΔE_{0e} is the excitation energy, and ($\mu_{ee} - \mu_{00}$) is the difference between the dipole moments of the ground and excited states. As discussed in the Supporting Information, the larger first hyperpolarizability of the protonated form cannot be explained by the $\mu_{0e}^2/\Delta E_{0e}^2$ term and should therefore be sought in the change in the dipole moment upon excitation. Indeed, this was confirmed by CIS/6-311G** calculations, which demonstrated that for model B, the ($\mu_{ee} - \mu_{00}$) term for the protonated form (−10.84 D) is ∼5 times larger than that for the deprotonated form (−2.02 D).

The effects of extending the model to account for the protein surroundings were estimated on the basis of TDHF and TDDFT calculations by considering the β_{HRS}(model D)/β_{HRS}(model B) ratio (Table 4). Increasing the size of the model leads to an enhancement of β_{HRS}, consistent with the experimental observation that the chromophore matrix has an important effect. At the TDHF level, this increase is on average ∼30% larger for the deprotonated form than for the protonated species. The situation is less clear at the TDDFT level. However, these surroundings effects do not modify the fact that the β_{HRS}(protonated)/β_{HRS}(deprotonated) ratio is larger than one.

Conclusions

We have systematically quantified the second-order nonlinear optical properties of Dronpa and EGFP by means of HRS. This technique is especially well suited for highly fluorescent molecules, since it accurately takes into account the contribution of MPF and does not overestimate the values of β. We have shown that the protonated form of Dronpa has a larger first hyperpolarizability than its deprotonated counterpart. We have ruled out the effect of resonance enhancement as an explanation for our counterintuitive observation of a larger β for the form with the higher transition energy. Theoretical calculations at different levels of sophistication show that the larger β for the protonated form of Dronpa is caused by the change in dipole moment upon excitation. The latter parameter is proportional to the first hyperpolarizability value and is ∼5 times larger for the protonated form than for the deprotonated form. These second-order nonlinear optical properties of GFP-like proteins become particularly important in the realm of combined nonlinear microscopy (two-photon fluorescence and second-harmonic generation) based on existing fusion proteins involving GFPs.

Supporting Information Available: Charts showing more complex models (E−H) used in the calculations and the different residues involved in the proton transfer in wt-GFP, experimental and calculated absorption spectra for Dronpa, experimental fluorescence spectrum of Dronpa at pH 8, a more elaborate account of the theoretical results with additional tables and figures, and complete ref 45. This material is available free of charge via the Internet at http://pubs.acs.org.

JA805171Q

(54) Marder, S. R.; Perry, J. W.; Tiemann, B. G.; Gorman, C. B.; Gilmour, S.; Biddle, S. L.; Bourhill, G. *J. Am. Chem. Soc.* **1993**, *115*, 2524–2526.
(55) Meyers, F.; Marder, S. R.; Pierce, B. M.; Bredas, J. L. *J. Am. Chem. Soc.* **1994**, *116*, 10703–10714.
(56) Kirtman, B.; Champagne, B.; Bishop, D. M. *J. Am. Chem. Soc.* **2000**, *122*, 8007–8012.